Journal of Hydrology xxx (2015) xxx–xxx

Contents lists available at ScienceDirect

Journal of Hydrology

journal homepage: www.elsevier.com/locate/jhydrol

The hydrological and environmental evolution of shallow Lake Melincué, central Argentinean Pampas, during the last millennium

Lucía Guerra [a,*], Eduardo L. Piovano [a], Francisco E. Córdoba [b], Florence Sylvestre [c], Sandra Damatto [d]

[a] Centro de Investigaciones en Ciencias de la Tierra (CICTERRA, CONICET-Universidad Nacional de Córdoba), Av. Vélez Sarsfield 1611, Ciudad Universitaria, Of.1, 2° Floor, X5016GCA Córdoba, Argentina
[b] Centro de Investigación y Transferencia de Jujuy (CIT, Jujuy-CONICET), Instituto de Geología y Minería, Universidad Nacional de Jujuy, Av. Bolivia 1661, San Salvador de Jujuy, Argentina
[c] Centre de Recherche et d'Enseignement de Géosciences de l'Environnement-CEREGE, Université Aix-Marseille, CNRS, IRD, Europôle méditerranéen de l'Arbois, BP 80, 13545 Aix-en-Provence cedex 4, France
[d] Laboratório de Radiometria Ambiental – Gerência de Metrologia das Radiações, Instituto de Pesquisas Energéticas e Nucleares – IPEN, Av. Prof. Lineu Prestes, 2242, São Paulo 05508000, Brazil

ARTICLE INFO

Article history:
Available online xxxx

Keywords:
Pampean Plains
Hydroclimatic changes
Paleoenvironmental reconstruction
Closed basin
Paleolimnological record
Last millennium

SUMMARY

Lake Melincué, located in the central Pampean Plains of Argentina, is a shallow (~4 m), subsaline lake (TDS > 2000 ppm), highly sensitive to hydrological changes. The modern shallow lake system is composed of: (a) a supralittoral area, which includes a narrow mudflat, a vegetated mudflat and wetlands subenvironments; and (b) the main water body, comprising lacustrine marginal and inner areas. The development and extension of these subenvironments are strongly conditioned upon lake surface fluctuations. Past environmental changes were reconstructed through sedimentological, physical and geochemical proxy analyses of two short sedimentary cores (~127 cm). Well-constrained ^{210}Pb ages profiles were modeled and radiocarbon chronologies were determined, covering a period from ~AD 800 to the present. The analyzed sedimentary cores from Lake Melincué allowed for the reconstruction of past hydrological scenarios and associated environmental variability, ranging from extremely low lake levels during dry phases to pronounced highstands at wet periods. The paleohydrological reconstruction revealed very shallow conditions in the period between AD 806 and AD 1880, which was registered by massive deposits with low organic matter. Relatively wetter phases disrupting this dry period were represented by organic matter increases. A major wet phase was registered by AD 1454, after the end of the Medieval Climate Anomaly. A subsequent abrupt shift from this wet phase to drier conditions could be matching the transition between the end of the Medieval Climatic Anomaly and the beginning of the Little Ice Age. The occurrence of sedimentary hiatuses between AD 1492 and AD 1880 in Melincué sequence could correspond to intensive droughts during the Little Ice Age. After AD 1880, banded and laminated, autochthonous, organic matter-rich sediments registered an important lacustrine transgression and the onset of a permanent shallow lake, corresponding to the beginning of the current warm period. The uppermost recent fine-grained, low salinity, organic sediments represent a lake transgression occurred in the 1970s, coeval with a general increase in precipitation across southeastern South America. This transgression is registered regionally in other Pampean lakes and in the 20th century instrumental records of Lake Melincué. This paleoenvironmental reconstruction provides a new high-resolution record that registers striking hydroclimatic changes occurred at a regional scale across the Pampean Plains during the last millennium and it contributes to understand the past climatic history in southeastern South America.

1. Introduction

Among the several natural archives with the potential to unravel past environmental variability in South America (Villalba et al., 2009), shallow, closed lakes are especially sensitive to changes in the hydrological balance, responding rapidly through marked

Abbreviations: CRS, Constant Rate of Supply; LIA, Little Ice Age; LSR, linear sedimentary rate; MCA, Medieval Climate Anomaly; SAM, South American Monsoon; SM, magnetic susceptibility; TOC, total organic carbon; TIC, Total Inorganic Carbon.

* Corresponding author. Tel.: +54 0351 5353800x30228.
E-mail address: luciaguerra83@gmail.com (L. Guerra).

http://dx.doi.org/10.1016/j.jhydrol.2015.01.002
0022-1694/

modifications in their physical, chemical and biological components. A growing number of studies highlight the value of sedimentological and geochemical analysis of closed-lake deposits for reconstructing past hydrological changes (e.g. Moreno et al., 2007; Valero-Garcés et al., 2003; Last and Ginn, 2005; Adrian et al., 2009; Steinman and Abbott, 2013).

Between 30° and 40°S, the Pampean region in central Argentina is characterized by the development of widespread shallow, closed lacustrine and swamp environments (Iriondo, 1989) with a wide range of water composition, salinities and trophic states (Quirós and Drago, 1999). Previous instrumental and historical studies revealed that Pampean hydrological systems have undergone important water level oscillations, mainly triggered by moisture changes (Cioccale, 1999; Pasquini et al., 2006; Piovano et al., 2009), which can be ascribed to the activity of the South American Monsoon (SAM) circulation system (Zhou and Lau, 1998; Vera et al., 2006; Garreaud et al., 2009). Within this geographical and climatic setting, paleolimnological research has focused on the areas north of 31°S (e.g. Lake Mar Chiquita; Piovano et al., 2002, 2004a, 2004b) and south of 37°S (e.g. Lagunas Encadenadas del Oeste de Buenos Aires; Córdoba, 2012; Lakes Nahuel Rucá and Loncoy, Stutz et al., 2010, 2012), revealing important hydrological changes throughout the late Holocene. However, a large unexplored area located between these latitudes has the potential to be a rich source of paleolimnological and paleoclimatological information. Therefore, understanding the magnitude and timing of late Holocene hydrological changes in these middle areas could be meaningful for regional correlation and cross validation of hydroclimatic reconstructions.

The sedimentary record of the closed and shallow Lake Melincué (33°S–61°W), provides an opportunity to unravel the history of past hydrological changes, covering the paucity of paleoclimatic data in the central area of the Pampean Plains during the late Holocene.

The overall goal of this paper is to provide a high resolution paleoenvironmental reconstruction for the last 1000 years in the central area of the Argentinean Pampas, through the integration of multiple sedimentological, physical and geochemical proxies. The study also identifies the hydrologic response of the lake system to large-scale climatic events during the late Holocene, such as the Little Ice Age (Bradley and Jones, 1993; Bradley et al., 2003; Villalba, 1994; Thompson et al., 1986), the Medieval Climate Anomaly (Villalba, 1994) and the current warm period (termed in Bird et al., 2011). Results here will contribute to the correlation of contrasting climatic stages in the last 1000 year evolution across the Pampean Plains, supplying information to understand the past activity of the South America monsoonal system.

2. Regional setting

The regional climate is temperate, subhumid–humid and mainly controlled by the South American Monsoon atmospheric system, which transports humidity from the Amazonian basin to extratropical latitudes via low level jet streams (Zhou and Lau, 2001; Vera et al., 2006; Garreaud et al., 2009; Fig. 1A). The mean annual precipitation is ~970 mm, with the maxima concentrated during the austral summer (December–March) and minima during the winter (June–September), following the seasonal activity of the atmospheric circulation. The lake is located north of the Arid Diagonal (Bruniard, 1982; Fig. 1A), which separates the region under the influence of the South American Monsoonal system, with prevailing summer precipitation, from the Westerlies circulation influence, with prevailing winter precipitation. The Arid Diagonal corresponds to a narrow band of low precipitation (<250 mm yr^{-1}) and extends in Argentina from the Atlantic coast at ca. 40–42°S up to the eastern flank of the Central Andes at 25–27°S.

Lake Melincué (33°S–61°W) is placed in an intracratonic basin in the Pampean Plain region (Fig. 1B). The lake is located within a NW–SE depression called "Pampa Hundida" (Pasotti et al., 1984), formed under flexural cortical and dynamic mantle effects (Pasotti et al., 1984; Brunetto et al., 2010; Dávila et al., 2010). Lake Melincué originated as a product of the low terrain morphology and damming of a drainage system, which had previously flowed to the east (Pasotti et al., 1984; Iriondo and Kröhling, 2007). The stratigraphy surrounding the lake is composed of an aeolian sedimentary succession deposited since the Pleistocene (Fig. 1B; Kröhling, 1999; Iriondo and Kröhling, 2007).

While the drainage basin has an extension of 680 km^2, the lake occupies a surface of ~60 km^2 (Fig. 1C). Currently (in 2013), the lake has a maximum water depth of ~4 m and has an ellipsoidal shape (east–west direction, ratio maximum longitude/maximum width = 1.6).

The primary source of water supplies is from unconfined outwash during episodic high precipitation; other supplies include a small permanent stream – El Pedernal – and groundwater. In order to reduce water level increases and flooding in the city of Melincué, water management began in the early 1940s, with the construction of the San Urbano channel, which reduces the upper catchment area (Fig. 1C; Peralta et al., 2003). To further control high water stands, lake water pumping started in 2004.

3. Materials and methods

The lake watershed and the present-day depositional environments were identified using Digital Elevation Models from USGS/NASA Shuttle Radar Topography Mission (Jarvis et al., 2008) and Landsat images (U.S. Geological Survey), and then mapped using Google Earth (Google inc. SRTM).

A standardized regional annual precipitation index for the 1899–2011 period was developed using the standardized mean annual precipitation records from twelve meteorological stations located up to 200 km from the lake (Marcos Juárez, Firmat, Nueve de Julio, Junín, Venado Tuerto, Rosario, Zavalla, Laboulaye, Los Cisnes, Pergamino, Oliveros and Canals; sources: National Meteorological Service, Instituto Nacional de Tecnología Agropecuaria; Fig. 1B), following methods used by Jones and Hulme (1996). The obtained precipitation index was then smoothed using a 5-term running average analysis to observe low frequency precipitation changes.

The annual lake water level record was reconstructed for the AD 1900–2013 period by compiling historical and instrumental data from different sources (Pasotti et al., 1984; Romano et al., 2005), as well as from personal communications of local observers.

A lake bathymetric map (m a.s.l.) was created with the information from 362 water depth points, measured in 2013 with a NAVMAN 4433 sonar. Surface sediment samples were collected with a dredge from 20 selected points. The mineralogy of efflorescence samples from the lake shore were determined by X-ray diffraction (Facultad de Ciencias Químicas, Universidad Nacional de Córdoba). Depth profiles of temperature (T, °C), total dissolved solids (TDS, ppm), electrical conductivity (EC, μS cm^{-1}), salinity (Sal., PSU) and dissolved oxygen (DO, ppm) were measured throughout the water column with a multiparameter probe.

Two short cores, M7B (length = 110 cm; 33°43′11.4″S/61°28′59.4″W) and M8B (length = 127 cm; 33°42′50.7″S/61°22′23″W), were retrieved from the deepest part of the lake in March 2011, using a Beaker-type sediment hand corer. The cores were stored at 4 °C and then split into two halves. Volumetric magnetic susceptibility (MS) was measured with a MS2E Bartington sensor every 0.5 cm on each core half. An initial core description was done following the criteria proposed by the Limnological Research Center Core

Please cite this article in press as: Guerra, L., et al. The hydrological and environmental evolution of shallow Lake Melincué, central Argentinean Pampas, during the last millennium. J. Hydrol. (2015), http://dx.doi.org/10.1016/j.jhydrol.2015.01.002

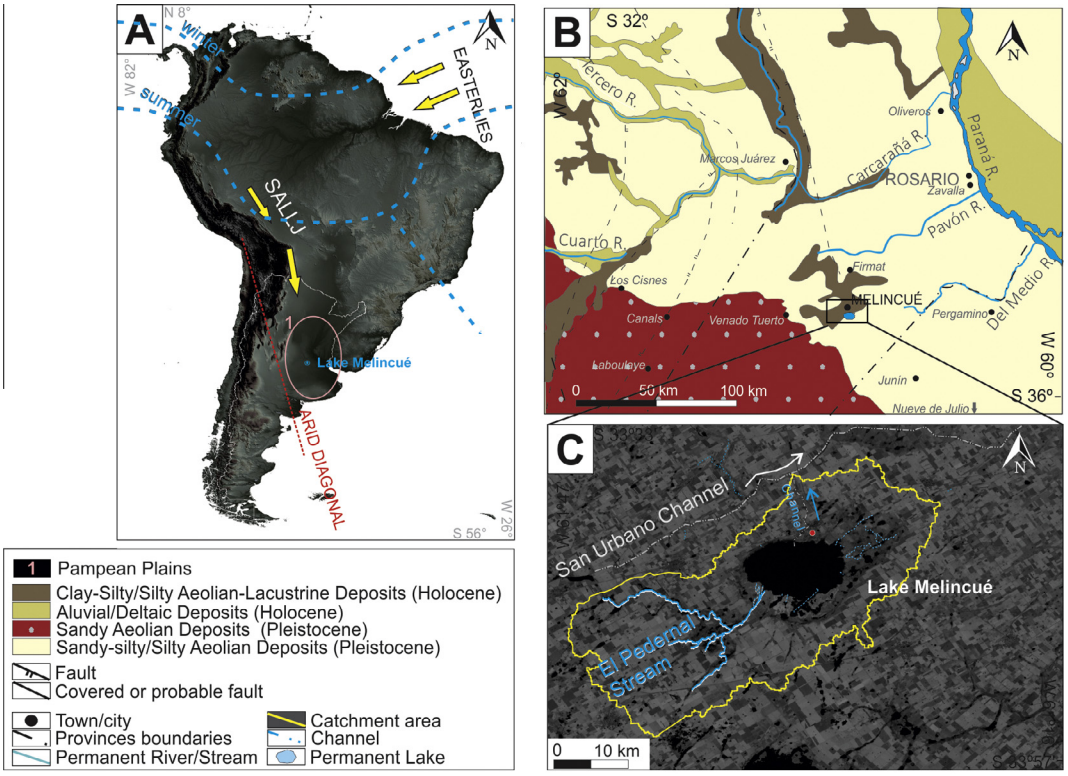

Fig. 1. Regional setting of the study area. (A) Schematic representation of the South American Monsoon system: location of the convergence zones in summer and winter (blue long-dashed lines), South American Low Level Jet (SALLJ), low level Easterlies, Arid Diagonal (red short-dashed line). (B) Geological map of the region; Lake Melincué is surrounded by aeolian and lacustrine silts deposits from the Pleistocene and Holocene. The black dots indicate the location of meteorological stations. (C) Landsat image (NASA, 2010) showing the Lake Melincué drainage basin. (For interpretation of the references to color in this figure legend, the reader is referred to the web version of this article.)

Facility (http://lrc.geo.umn.edu/laccore/icd.html). Samples were taken every 1 cm or 2 cm, limited by macroscopic sedimentological and MS changes.

Subsamples ($n = 49$) for grain size analysis were pre-treated with H_2O_2 (30%) for organic matter removal, and with HCl (10% for 24 h) to eliminate carbonates. Mean particle sizes were determined on both surface and core samples with an HORIBA LA950 laser scattering analyzer.

Total nitrogen (TN), total carbon and total organic carbon (TOC) percentages were determined by combustion and chromatography separation in a CNS elemental analyzer (NA Fisons) at CEREGE (Centre Européen de Recherche et d'Enseignement des Géosciences de l'Environnement, Aix-en-Provence, France), following the method proposed by Verardo et al. (1990). Subsamples for TOC were previously decarbonated (10% HCl). Total Inorganic Carbon (TIC) was then calculated by subtracting TOC from the total carbon. TOC/TN ratio was employed as an additional indicator in the analyses. Obtained variables were analyzed through principal component analysis (PCA).

The radiocarbon chronology of twelve organic-rich samples (5 from M7B and 7 from M8B) was obtained via Accelerator Mass Spectrometry (AMS) at the NSF-Arizona AMS Laboratory (Tucson, USA). Ages were calibrated using the Calib 7.0 software package (Stuiver and Reimer, 1993) and modeled with the SHCal13 curve (Hogg et al., 2013), selecting medians of the 95.4% distribution (2σ probability interval).

Radionuclides of ^{210}Pb were measured at the Instituto de Pesquisas Energéticas e Nucleares (IPEN, Sao Paulo, Brazil) in order to date the recent sediments. The uppermost 70 cm of duplicated cores (M7A and M8A) was sampled at ~2 cm interval or at every visible sedimentary change. The analytical determination was based on radiochemical separation of the sample, gross alpha counting, for ^{226}Ra (Oliveira, 1993), and gross beta activity, for ^{210}Pb concentrations, which were measured on a proportional detector of low background radiation Berthold LB 770 (Moreira, 1993). The procedures are detailed by Piovano et al. (2002). Unsupported ^{210}Pb activity was calibrated using the Constant Rate of Supply model (CRS; Appleby, 2008) to calculate sediment ages, following Sanchez-Cabeza and Ruiz-Fernández (2012) and Binford (1990).

4. Results

4.1. Hydroclimatic variability and limnology

Regional rainfall is characterized by a marked temporal variability and controls the hydrological balance of the Lake Melincué. The close connection during the 20th century between regional annual precipitation index and lake water-level variability is presented in Fig. 2A and B. These graphs show that low regional precipitation index and low lake-stands dominated from AD 1900 to 1970s. In the 1970s, a shift toward precipitation increases led to important rises in water level. The highest recorded lake level, 86.15 m a.s.l., was reached in 2003; after this maximum, the lake started to retreat.

Water-level modifications produce large surface variability over the flat geomorphology of the lacustrine system and its surrounding area. Reduced lake areas are developed during the lowstands (e.g., 60 km^2 in AD 1972; Fig. 2C), while considerable larger extensions characterize the highstands (e.g. 145 km^2 in AD 2003; Fig. 2C). Lake expansions have provoked important floods, which have affected most of infrastructure surrounding the lake (roads, farmlands, towns and tourism infrastructure) as well as part of the city of Melincué. Most of the affected engineering was located

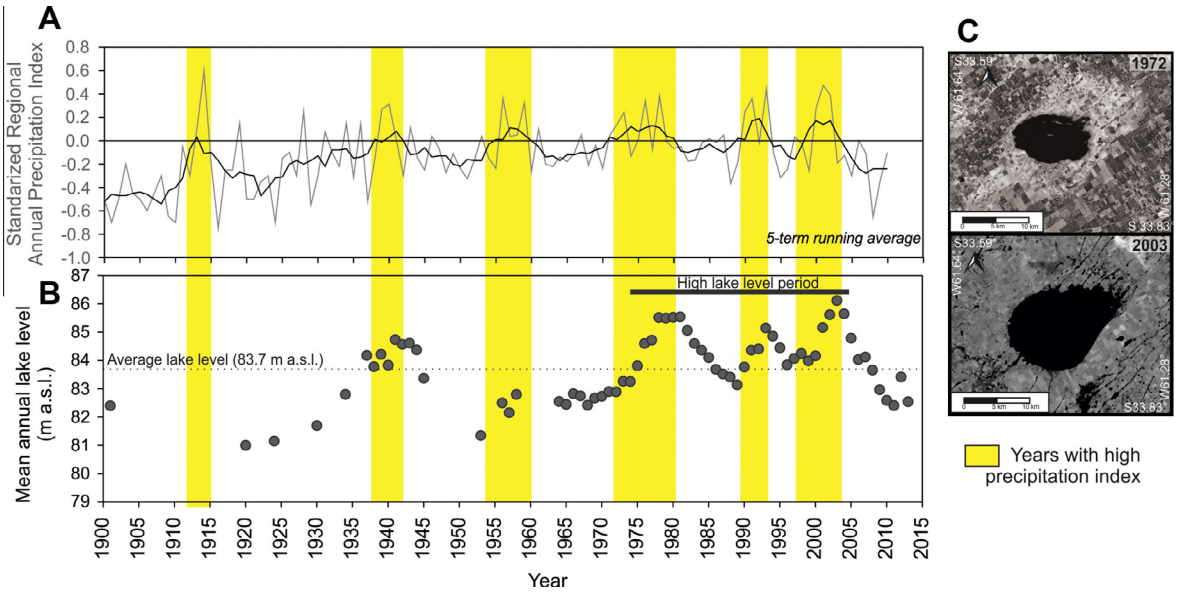

Fig. 2. Precipitation and lake-level variability during the 20th century. (A) Standardized regional annual precipitation index (gray line) and smoothed values of the temporal series (black line; 5-term running average). The index was calculated for the period 1899–2011, from 12 precipitation stations (distance to Melincué <200 km). Yellow shaded bars indicate positive smoothed precipitation indexes. (B) Lake Melincué mean annual water level (m a.s.l.) reconstructed through data from different sources (Romano et al., 2005; Pasotti et al., 1984 and personal communication of local observers). Average water level is marked with a dashed line. The length of the last high lake level period is indicated with a horizontal bar. (C) Satellite Landsat images (NASA) showing the lake surface in contrasting low (1972) and high (2003) lake level-stands. (For interpretation of the references to color in this figure legend, the reader is referred to the web version of this article.)

near the lake; since it was constructed in low topographic levels during lowstand periods (i.e., during the late 19th century).

On a north–south transect, the lake morphology is characterized by a low gradient shallow zone, where coarsed-grain sediments accumulate, and a deep and flat depocenter where finer sediments are deposited (Fig. 3). In the southwestern lake-shore a small permanent stream, El Pedernal, flows into the lake.

The lake is polymictic, without significant vertical thermal stratification (according to March 2011 and April 2013 measurements; Fig. 4), which is a common characteristic of Pampean lakes (Quirós et al., 2002; Iriondo, 1989) due to a combination of low depths and intense winds. Lake water is subsaline (i.e., TDS = 2077 ppm; EC = 4155.83 μS cm^{-1}) and alkaline (pH = 9.56; Fig. 4). Nevertheless, chemical composition can be modified by lake

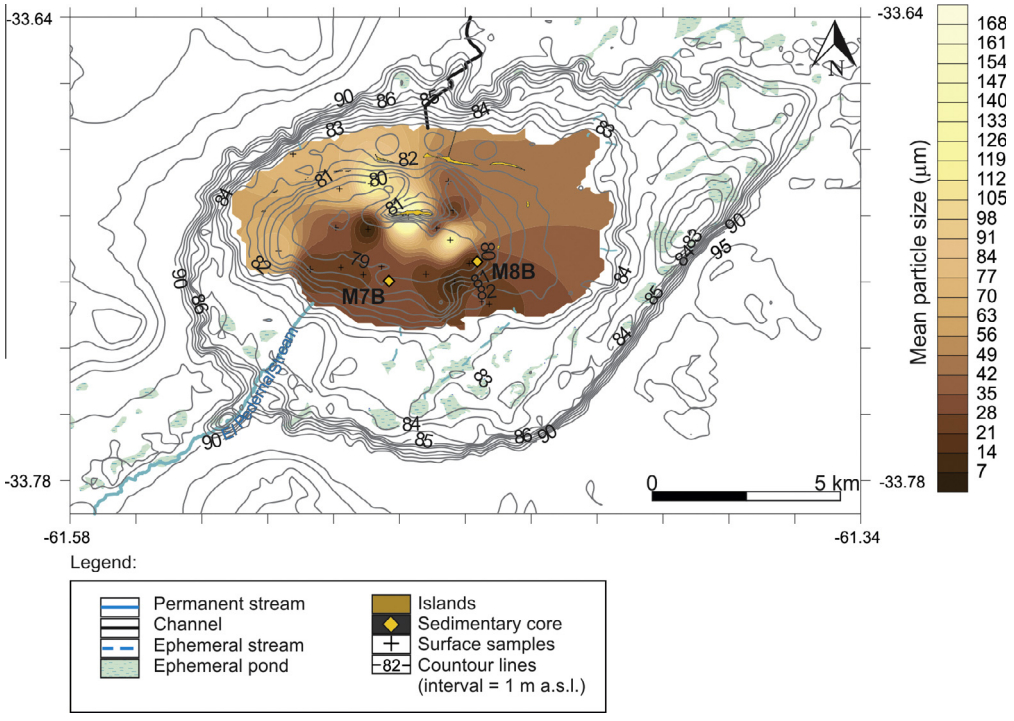

Fig. 3. Bathymetry map and grain-size distribution of the superficial sediments of Lake Melincué. Elevation contour lines are marked with gray lines (contour interval = 1 m a.s.l.). The grid map of the mean particle size is based on 49 superficial lacustrine samples (Krigging interpolation method); light yellow colors represent coarser material while dark brown colors indicate finer sediments. The locations of sedimentary cores (M7B and M8B) are indicated. (For interpretation of the references to color in this figure legend, the reader is referred to the web version of this article.)

Please cite this article in press as: Guerra, L., et al. The hydrological and environmental evolution of shallow Lake Melincué, central Argentinean Pampas, during the last millennium. J. Hydrol. (2015), http://dx.doi.org/10.1016/j.jhydrol.2015.01.002

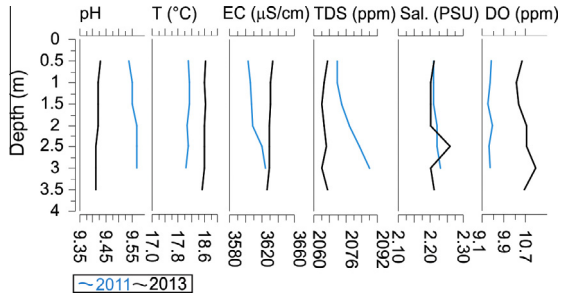

Fig. 4. Vertical profiles of chemical and physical water properties of Lake Melincué in March 2011 and April 2013, including pH, temperature (T, °C), electrical conductivity (EC, µS/cm), total dissolved solids (TDS, ppm), salinity (Sal., PSU), dissolved oxygen (DO, ppm). Note the absence of significant water stratiphication in both samplings.

level oscillations. For instance, while in 2011 the composition was bicarbonate, sodium and chloride-rich, by 2013 the composition became only bicarbonate and sodium-rich (unpublished results).

4.2. Present day depositional subenvironments

The modern shallow lake system is composed of: (a) a supralittoral area, which includes a narrow mudflat, a vegetated mudflat and wetlands subenvironments; and (b) the main water body, that includes lacustrine marginal and lacustrine inner areas (Fig. 5A).

The supralittoral area is bounded by the lake shoreline and reaches a maximum extension during lowstands (Fig. 5B) and a minimum, during highstands (Fig. 5C). The mudflat subenvironment is similar to those described in other closed lacustrine systems (Hardie et al., 1978; Piovano et al., 2002; Last and Ginn, 2005; Zanor et al., 2013, among others). It is confined to a narrow area around the lake (Fig. 5D) characterized by thin (<1 cm), puffy and porous efflorescent crusts, which are mainly composed of burkeite $Na_6(CO_3)(SO_4)_2$ (Fig. 5E and F). These types of crusts are produced when subsurface brines are drawn to the surface by evaporative pumping or by evaporative concentration (Hardie et al., 1978; Eugster, 1980; Last and Ginn, 2005). Cracking structures can be found locally in this subenvironment (Fig. 5E). The mudflat is surrounded by a vegetated mudflat (Fig. 5G), where saline crusts are also developed but some hallophilous vegetation (e.g., *Distichlis spicata* and *Paspalum vaginatum*; Romano et al., 2005) grows forming patches. The wetlands are developed in a low gradient zone around the lake with a dominant SW–NE direction; this area is currently under intense anthropogenic stress (Fig. 5H and I).

The mudflat is formed only during low water level conditions (Fig. 5B), and thus, higher salinities. During higher levels (e.g. in 2003; Fig. 5C), ion concentration of lake water is diluted precluding the evaporites precipitation. As a result, mudflats become flooded and the lake system is composed of only the main water body and the wetlands.

Within the main body of water, the lacustrine marginal subenvironment is formed on a low slope zone, located between the present day shoreline and the inner area (Fig. 5A). It is composed of a coarse silts and fine sands, hard substratum (Fig. 3) that corresponds to the submerged continuation of the supralittoral area. Within the marginal area, some topographic highs parallel to the lake shore are emerged, forming islands (Fig. 5B, C and J).

The inner lacustrine area occupies the flat, distal and deepest zone of the lake (Fig. 5A). This area has been submerged for the majority of the time for which instrumental information is available. Relatively high slopes separate the inner areas from the shallow marginal zone. Pelagic deposits are composed of dark, soft, very fine to medium silt (Fig. 3).

Current low stand conditions allow for the development of all the described subenvironments. Lake expansion–contraction cycles, however, can re-shape these subenvironments, causing marked lateral shifts in their limits.

4.3. Sedimentary cores and paleoenvironmental interpretation

4.3.1. Sedimentology and proxies' description

Through first core description two main sections can be identified: a basal massive and compact sediment below the ~70/75 cm depth (M7B/M8B) and an uppermost section composed of banded (>1 cm) and laminated (<1 cm) sediments (Fig. 6).

A distinctive dark, massive layer stands out from both cores between 83/90 cm and 93/96 cm (M7B/M8B).

High resolution sedimentological and multiple proxies indicate significant changes along the sedimentary sequence of Lake Melincué (Fig. 6). Overall, MS ranges from 3.5 to 133.5 SI, showing the highest values in the lower portions, below the 72/76 cm level (M7B/M8B). Mean particle size varies between 14 and 59 µm; the coarsest sediments are found in the middle sections of both cores, while the finest material characterizes the top of the cores (uppermost 30 cm). TIC percentages reach up to 2.00%. The TOC and TN percentages range from 0.01% to 0.25% and from 0.44% to 2.73%, respectively, and they positively covary along the cores. TOC/TN ratios range from 10.27 to 35.00, showing a major shift at ~70 cm.

Multivariate principal components analysis (PCA) provides a broad view of the relationships among TOC, TN, TIC, TOC/TN ratios, MS and mean particle size of the samples (Fig. 7A and B). Two principal components, (PC1 and PC2) can be identified accounting for 46.15% and 26.29% of the variance, respectively.

PC1 shows a significant negative correlation with TN and TOC, while it correlates positively with TOC/TN values (Fig. 7A). Results suggest that this component is related to the organic matter source, allowing for the distinction between allochthonous and autochthonous origins (Fig. 7B; Meyers and Lallier-Vergès, 1999; Meyers, 1994, 2003).

PC2, on the other hand, has a positive correlation with TIC and mean particle size, but a negative correlation with MS and TOC/TN ratio. Results suggest that PC2 groups samples according to the water salinity and carbonates precipitation. Almost no correlation is observed in the biplot between TIC and the organic proxies TN and TOC; (Fig. 7B).

4.3.2. Sedimentary facies

Based on the sedimentary attributes, the analysis of physical properties and geochemistry, seven sedimentary facies (F1–F7; Table 1; Figs. 6 and 8) are defined, representing the record of diverse paleolimnological conditions. Average values of measured variables and the synthesis of paleoenvironmental interpretation for each facies are detailed in Table 1. Facies are described following their position in the core, from base to top. The description includes the most diagnostic paleoenvironmental parameters.

F5 and F6 are composed of massive sediments (Figs. 6, 8A and B) with low organic matter proportion (TOC < 1%) and a TOC/TN ratio >20, indicative of terrestrial contribution (Table 1; Meyers, 1994; Meyers and Teranes, 2002). They are associated with high TIC percentages (~0.6%) and thus, with high water salinity. This interpretation is supported by the PCA results, which groups the F5 and F6 facies near the TIC curve and the PC2 positive end (Fig. 7B). F5 is interpreted as mudflat deposits, which occasionally can be flooded by very shallow water bodies. Higher organic matter percentages found in F6 (maximum of up to 1.81%; Fig. 6) could be caused by higher inputs of terrestrial organic matter under shallow lake water levels.

Please cite this article in press as: Guerra, L., et al. The hydrological and environmental evolution of shallow Lake Melincué, central Argentinean Pampas, during the last millennium. J. Hydrol. (2015), http://dx.doi.org/10.1016/j.jhydrol.2015.01.002

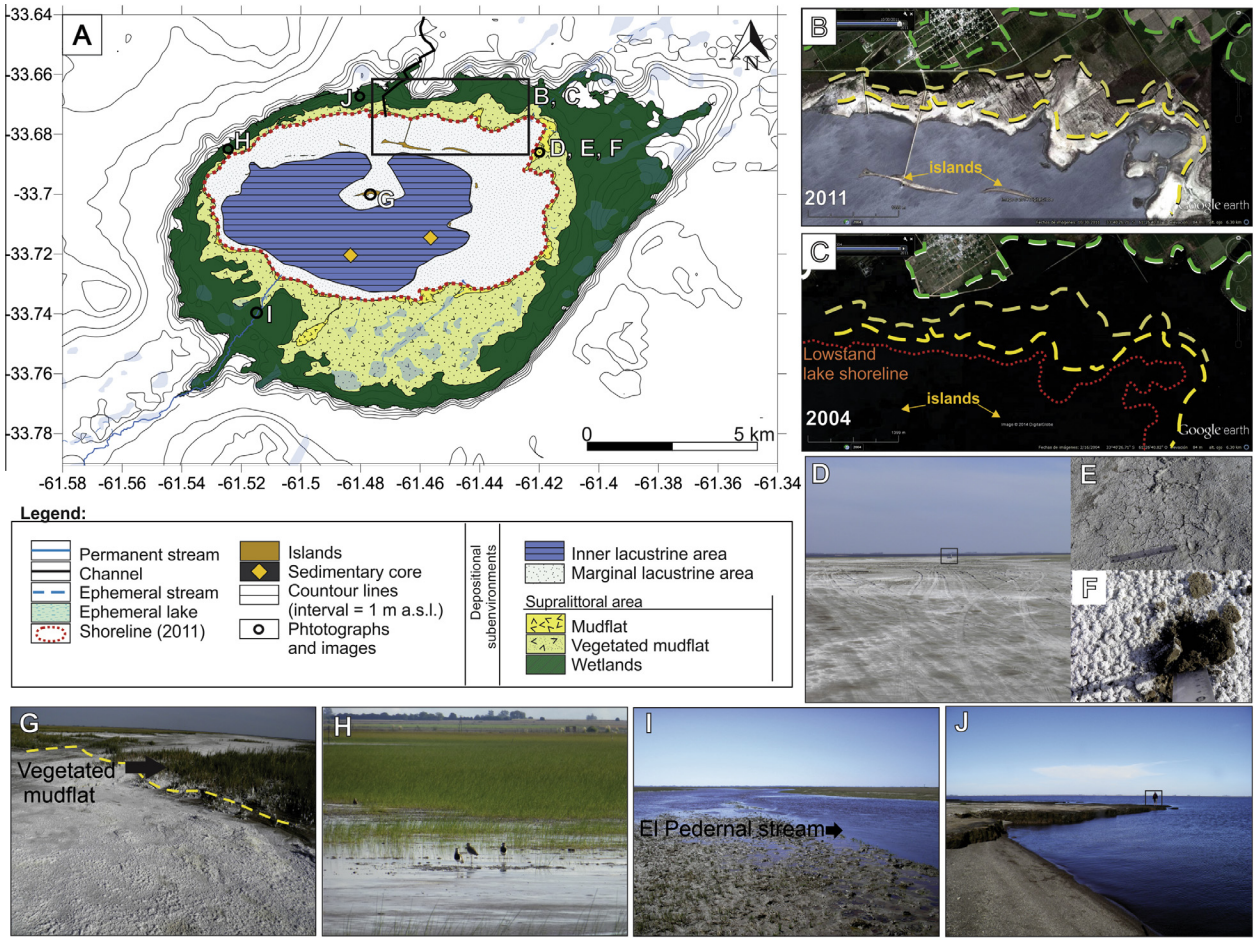

Fig. 5. Present-day sedimentary subenvironments in Lake Melincué system during a low lake level stage. (A) Map of the depositional subenvironments recognized in 2011; letters (B–J) indicate the location of the corresponding pictures; black rectangle indicates the location of B and C satellite images. (B) Google Earth satellite image from 2011 showing a low lake level scenario. (C) Satellite image from 2004 showing a high lake level stage. The mudflat and vegetated mudflat subenvironments are developed during the low level stage (2011) while they become flooded during the highstand (2004). (D) Mudflat subenvironment, rectangle shows a vehicle as scale. (E) Cracking structures in the mudflats. (F) Efflorescent saline crusts in the mudflats. (G) Vegetated mudflat. (H) Wetlands. (I) El Pedernal stream near its mouth in the wetland area. (J) Island located in the marginal area, the rectangle shows a person as scale.

F7 is composed of black, massive (Fig. 8A), organic-rich muds (TOC = 1.3%; mean particle size = 21.56 μm; Table 1) with a predominantly terrestrial organic matter source (TOC/TN > 20). Organic-rich sediments show low TIC percentages (~0.33%), suggesting the development of a subsaline lake of intermediate to high water depth, with a dominant input of allochthonous organic matter.

F5, F6 and F7 display high MS values (>30 SI), which could be favored by low dilution from poor organic components and magnetic material preservation in an oxidant shallow environment (Dearing, 1999).

F4 is formed by banded (Fig. 8C) light/dark gray, organic-rich (>2%) coarse silts (32.39 μm; Table 1). Coarse particles reveal a high competence clastic flux into the lake. TOC/TN ratios ~14 indicate mixed terrestrial and algal organic matter (Meyers, 1994; Meyers and Teranes, 2002). Minimum MS values (13.78 SI) in this facies could be explained by a dilution of the magnetic signal by high organic matter proportion, and magnetic dissolution processes in anoxic bottom conditions (Karlin and Levi, 1983; Dearing, 1994). High TIC percentages (0.52%) point toward evaporitic precipitation in saline waters (Fig. 7). Based on these evidences, F4 can be interpreted as the deposit of an intermediate to deep, saline and highly productive lake.

F2 and F3 form thick sets (>5 cm) of finely laminated sediments (<1 mm; Fig. 8D). F3 is formed by light gray, well preserved, finely laminated silts with carbonates (TIC ~0.5%) and high TOC ~1.4% (Table 1). Combined sedimentological and geochemical variables indicate that deposition took place under shallow to intermediate lake levels, high salinities and high primary productivity.

F2, in turn, is formed by dark-brown, finely laminated (Fig. 8D and E), medium to fine silts with low TIC percentages (0.26%; Table 1). Fine particle sizes reveal a low-energy, deep depositional environment, while low carbonate amounts indicate comparatively lower water salinities regarding F3.

Alternating F2 (dark with marked lamination) and F1 (light and faintly laminated) are developed along the uppermost part for the core (Figs. 7 and 8E). These organic matter-rich facies (TN = 0.1%; TOC ~ 1.3–1.5%; TOC/TN ~14; Table 1; Fig. 5) can indicate high internal productivity (e.g. Mayr et al., 2005). An association of both facies with the organic proxies (TN and TOC) on the negative end of PC1 in the distribution biplot (Fig. 7B) supports this interpretation. Finer particles and better-developed lamination in F2 indicate a quieter deposition and thus, comparatively higher lake levels than F1.

4.3.3. Sedimentary units

Based on the vertical arrangement of the distinctive identified facies, three main sedimentary units are defined in the sedimentary sequence: unit A (UA), unit B (UB) and unit C (UC; Fig. 6). The paleoenvironmental evolution of the lake system and associated hydrological changes can be reconstructed from each unit.

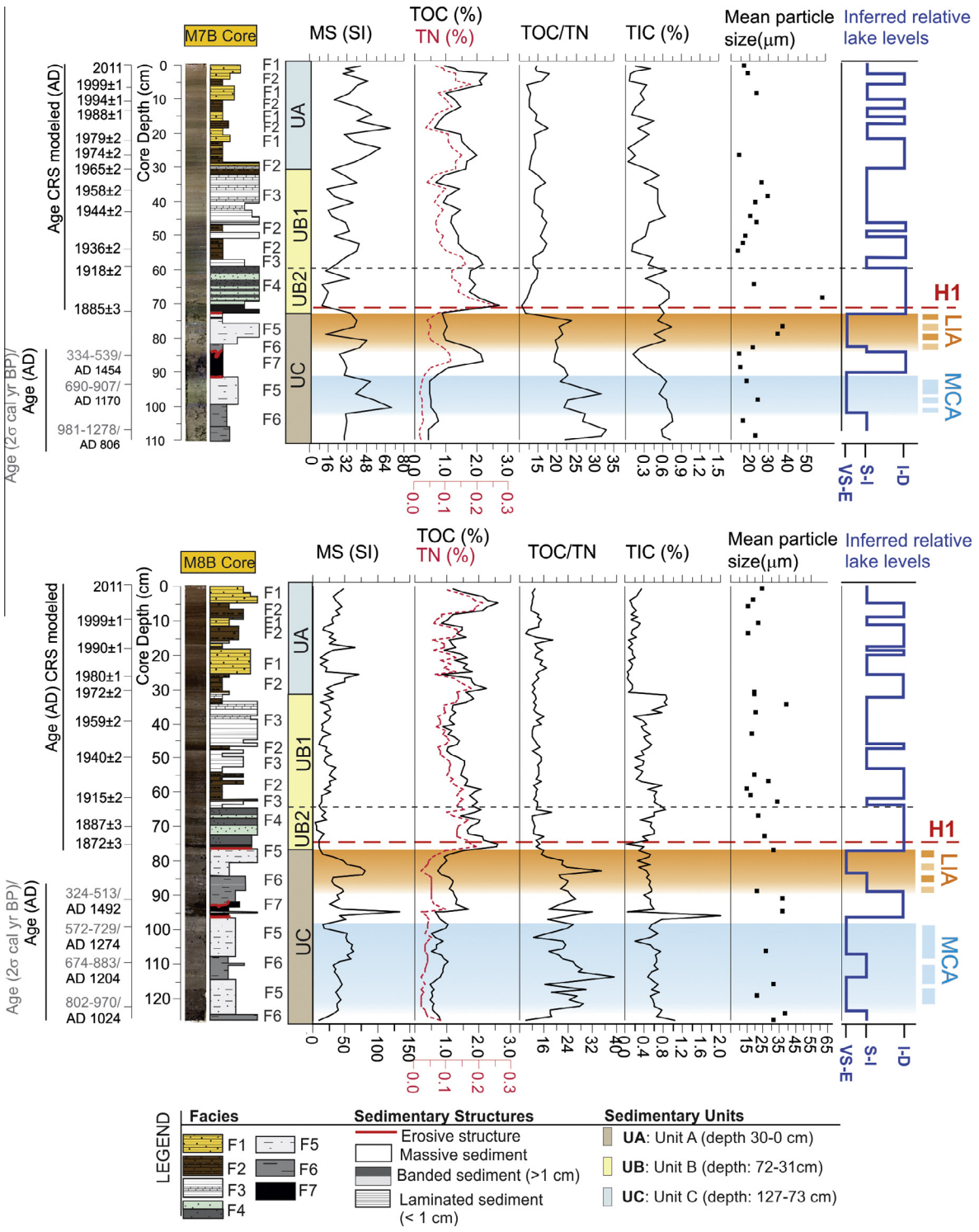

Fig. 6. Multi-proxy data of M7B (upper part) and M8B (lower part) sedimentary cores from Lake Melincué and water level changes. From left to right: ^{210}Pb (upper sections) and ^{14}C (lower sections) ages, core depths (cm), core photographs, sedimentary facies, sedimentary units, magnetic susceptibility (MS; SI), total organic carbon (TOC, full line) and total nitrogen (TN, dashed line) percentages, TOC/TN ratios, TIC percentages, mean particle sizes (μm), and relative lake levels. ^{14}C ages are presented in cal. yr BP with the 2σ error and the median age (AD). ^{210}Pb ages were obtained through the CRS model. Shaded horizontal bars highlight high organic carbon levels. Relative lake levels (very shallow to ephemeral –VS-E–; shallow to intermediate –S-I–; intermediate to deep –I-D–) are inferred in base to the identified facies. Medieval Climate Anomaly (MCA) and Little Ice Age periods (LIA) are shaded. H1 indicates the settlement of Melincué agricultural village at the end of the 19th century.

Units are easily recognizable by macroscopic sedimentological discontinuities and marked shifts in the analyzed proxies.

4.3.3.1. Unit C. This unit extends from the base of the cores up to a sharp contact at 72/76 cm depth (in M7B/M8B; Fig. 6) and it is composed of F5, F6 and F7 facies. It is recognizable at a macroscopic scale as massive and compact gray sediments (Fig. 8A and B). Geochemically, it is characterized by TOC/TN ratios >20, which reflects a dominant terrestrial source of the scarce organic matter (Meyers, 1994; Meyers and Teranes, 2002).

Please cite this article in press as: Guerra, L., et al. The hydrological and environmental evolution of shallow Lake Melincué, central Argentinean Pampas, during the last millennium. J. Hydrol. (2015), http://dx.doi.org/10.1016/j.jhydrol.2015.01.002

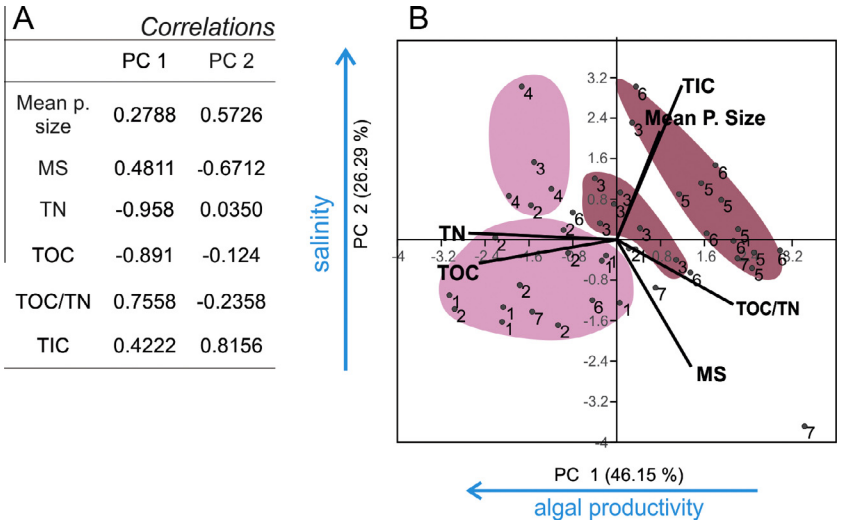

Fig. 7. Principal component analysis. Dataset includes: TN, TOC, MS, TIC, TOC/TN ratios, and mean particle size (Mean p. size); 49 cases were analyzed. (A) Correlation coefficients between variables and the first two principal components. (B) PCA biplot and samples' distribution (dots). The first PCA indicate the organic matter source, and the second PCA groups the samples according to water salinity. Numbers correspond to facies (1–7) and shadowed areas group them according to their distribution in the biplot.

Table 1
Facies description, proxies and paleoenvironmental interpretations. From left to right, columns contain: the facies code; a synthetic description; mean values of the measured variables – TOC, TN and TIC (%), TOC/TN ratios, MS (SI units) and mean particle sizes (μm); and the inferred lake level and paleoenvironmental characteristics.

	Facies	Variables (mean values)		Inferred lake level and paleoenvironmental characteristics
F1	Ochre, faintly laminated, organic-rich, medium silts	TOC = 1.29% TN = 0.11% TIC = 0.19%	TOC/TN = 14.16 MS = 34.3 $*$ 10^{-5} SI Mean particle size = 20.5 μm	Intermediate to shallow, perennial subsaline lake with high algal productivity
F2	Dark-brown, finely laminated, organic-rich, medium to fine silts	TOC = 1.55% TN = 0.11% TIC = 0.26%	TOC/TN = 13.84 MS = 33.54 $*$ 10^{-5} SI Mean particle size = 17.73 μm	Deep, perennial subsaline lake with low energy sedimentation and high algal productivity
F3	Light gray, finely laminated, organic-rich medium silt with carbonates	TOC = 1.37% TN = 0.10% TIC = 0.49%	TOC/TN = 13.92 MS = 24.13 $*$ 10^{-5} SI Mean particle size = 25.45 μm	Shallow, perennial saline lake with carbonate precipitation
F4	Light/dark gray, banded, organic-rich coarse silts with carbonates	TOC = 1.96% TN = 0.15% TIC = 0.52%	TOC/TN = 13.78 MS = 13.78 $*$ 10^{-5} SI Mean particle size = 32.39 μm	Intermediate to deep, perennial saline lake, with high algal productivity and detritic input (high competence transport). Anoxic bottom
F5	Gray, massive and compact, highly magnetic, medium to coarse silts with carbonates	TOC = 0.70% TN = 0.03% TIC = 0.61%	TOC/TN = 22.9 MS = 47.04 $*$ 10^{-5} SI Mean particle size = 26.85 μm	Very shallow to ephemeral saline lake with low algal productivity. Probable subaerial exposures
F6	Light gray, massive and compact, silt with carbonates and organic matter	TOC = 0.97% TN = 0.05% TIC = 0.58%	TOC/TN = 22.89 MS = 34.4 $*$ 10^{-5} SI Mean particle size = 27.91 μm	Shallow saline lake with relatively higher terrestrial organic supplies
F7	Black, massive organic-rich mud	TOC = 1.40% TN = 0.06% TIC = 0.33%	TOC/TN = 21.53 MS = 36.8 $*$ 10^{-5} SI Mean particle size = 21.56 μm	Intermediate to deep subsaline lake, with terrestrial organic matter input

At the base of the unit, massive and compact silts from F5 alternate with relatively organic-richer facies from F6. The alternation represents the record of fluctuating hydrological scenarios between very shallow or ephemeral water bodies, fringed by mudflats (F5), and comparatively, higher water level environments (F6).

At 85/95 cm depth (in M7B/M8B), above an irregular contact, it overlies the organic-rich F7, denoting a period of lacustrine transgression and high organic matter accumulation. The top of F7 is also cut by a sharp and irregular contact that might have been caused by erosive processes which took place during subaerial exposures under pronounced droughts. Overlying F7, alternating F5/F6 indicates the return of very shallow water levels.

Massive and homogeneous sediments throughout UC can be ascribed to sediment mixing/reworking, which are evident in the present-day mudflats: halophyte vegetation growth, activity of organisms tolerant to salinity, precipitation–desiccation of saline minerals, cracking, and wind action.

4.3.3.2. Unit B. An abrupt drop of MS and TOC/TN values and increased organic matter percentages mark the base of UB at

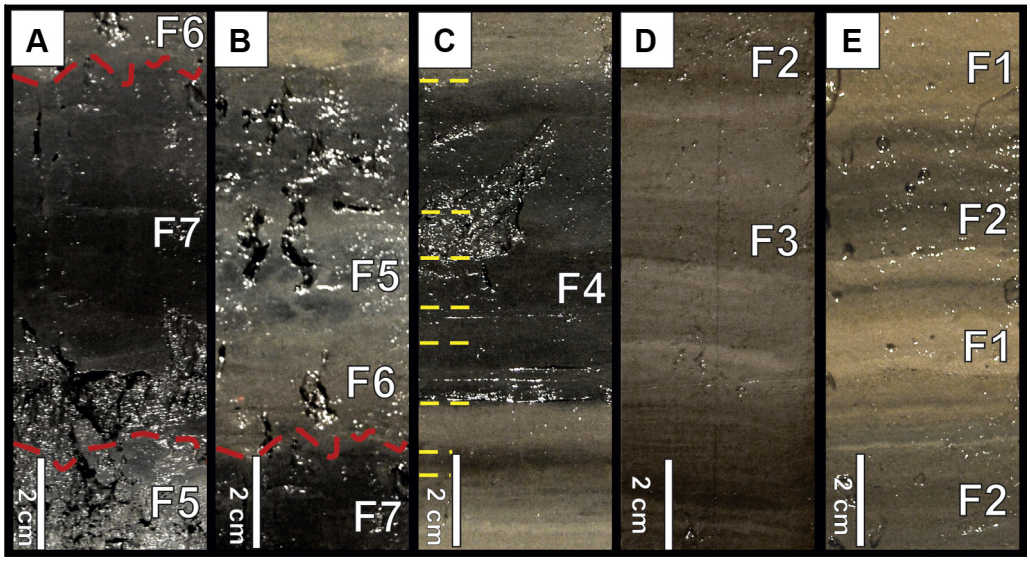

Fig. 8. Detailed photographs of the identified sedimentary facies (F1–F7) from Lake Melincué sequence. (A) F5, F6 and F7 intercalation; (B) sets of F7, F5 and F6; (C) banded F4; (D) F3 and F2; (E) F2 and F1 intercalation. Light colored (yellow), dashed lines mark different banding structures and dark-colored (red), dashed lines indicate erosive structures. (For interpretation of the references to color in this figure legend, the reader is referred to the web version of this article.)

72/76 cm depth (M7B/M8B), highlighting a remarkable change in the limnology of Lake Melincué. The drop in the TOC/TN ratio to values <14 suggests a shift in the major origin of the organic matter, from predominantly terrestrial plants in UC to mixed organic sources. The well-defined laminations and bands that extend along UB, without visible discontinuities, reflect a deeper water column and perennial lacustrine conditions.

UB is composed of F4, F3 and F2 sets and can be separated in subunits UB1 and UB2. UB2 extends from the base of the unit up to 60/65 cm depth (M7B/M8B; Fig. 6). It is formed by banded organic-rich sediments from F4, which record an important lake transgression, promoting primary organic productivity. At 60/63 cm (M7/M8) the initial deposition of subunit UB1 indicate a new lake expansion. Sediments from UB1 grading upward from F2 to F3 facies (Fig. 6), indicate declination in the lake internal productivity and raising salinities. This trend evidences a gradual lake contraction toward the top of the subunit.

4.3.3.3. Unit A. The onset of Unit A at 30/33 cm level (M7B/M8B; Fig. 6) is marked by an increase of organic matter contents, and significant TIC drop. The unit is composed of organic-rich, fine silts sets formed by alternating F1 and F2, indicating the development of high lake level conditions, lower salinities and high primary productivity.

5. Chronology

The chronology of Lake Melincué cores was based on ^{210}Pb and AMS ^{14}C dating (Fig. 9). The ^{14}C chronology was applied in the lower part of the cores. These results are shown in Table 2. The sediments of Lake Melincué reflect the history of the last millennia. The oldest age reached is 1144 ± 78 cal. yr BP/AD 806 (Fig. 9) at the 108 cm level at the base of M7B.

The chronological results show age reversals in UB (Fig. 9; Table 2). Since the anomalous ages were obtained from samples with low TOC/TN ratios (<20), which indicate the presence of lacustrine organic matter (Meyers, 1994, 2003), a bias could be introduced due to a potential reservoir effect. Thus, five radiocarbon ages derived from UB samples were rejected (two in M7B and three in M8B; Table 2; Fig. 9), and the ^{14}C chronological framework was built using samples from UC, which are characterized by dominant terrestrial organic matter sources. Distinctive sedimentary features were used to crosscheck the dates from both cores. For example, lithologically correlated F7 was dated by 496 ± 48 cal. yr BP/AD 1454 at 86.5 cm in M7B, and 458 ± 59 cal. yr BP/AD 1492 at 91.5 cm in M8B.

Linear regressions were applied in order to estimate a minimum sedimentation rate in UC sediments. Minimum linear sedimentation rates (LSR) of 0.04 and 0.07 cm yr^{-1} were estimated for UC dated sediments from M7B and M8B, respectively (Fig. 9). Extremely low sedimentary rates found in M7B could indicate the presence of overlooked hiatuses within the core. Comparable sedimentary rates were reported in other shallow, saline Pampean lakes for the same temporal period (0.02 cm yr^{-1}; Córdoba, 2012).

A high resolution chronological framework for Units B and A was obtained through the ^{210}Pb dating method (Fig. 9). The oldest limit reached with the CRS model (Appleby and Oldfield, 1978; Robbins, 1978) in M8C and M7C cores corresponds to AD 1859 ± 4 (at ~78 cm) and AD 1832 ± 5 (at 78 cm depth), respectively. Since modeled ^{210}Pb ages must be validated against independent stratigraphic markers of a known age (e.g. Appleby, 2008; Arnaud et al., 2002; Von Gunten et al., 2009), two stratigraphic markers were selected to control the upper (UA) and lowermost (UB) parts of the ^{210}Pb dated sediments. Previous paleolimnological studies on Pampean lakes have recognized significant correlations between sedimentary facies and lake-level changes (Piovano et al., 2002, 2004a, 2004b, 2009). Sedimentary organic matter variation was used to reconstruct the primary productivity and lake water-level changes controlled by hydroclimatic variability (Piovano et al., 2002; da Silva et al., 2008; Córdoba, 2012). Therefore, stratigraphic markers were defined as organic matter-rich levels associated with high lake productivity and wet phases. The marker of AD 1976 ± 4 was chosen to control the younger ^{210}Pb derived dates. It corresponds to an uppermost organic carbon-rich mud accumulated by 1976 matching the most noticeable lake highstand occurred during the 20th century, registered on instrumental and paleolimnological records across the Pampean Plains (Pasquini et al., 2006; Piovano et al., 2009; Córdoba, 2012).

The oldest stratigraphic marker corresponds to AD 1878 ± 10. It was validated against documentary and instrumental evidences, which indicate precipitation increases for the corresponding

Please cite this article in press as: Guerra, L., et al. The hydrological and environmental evolution of shallow Lake Melincué, central Argentinean Pampas, during the last millennium. J. Hydrol. (2015), http://dx.doi.org/10.1016/j.jhydrol.2015.01.002

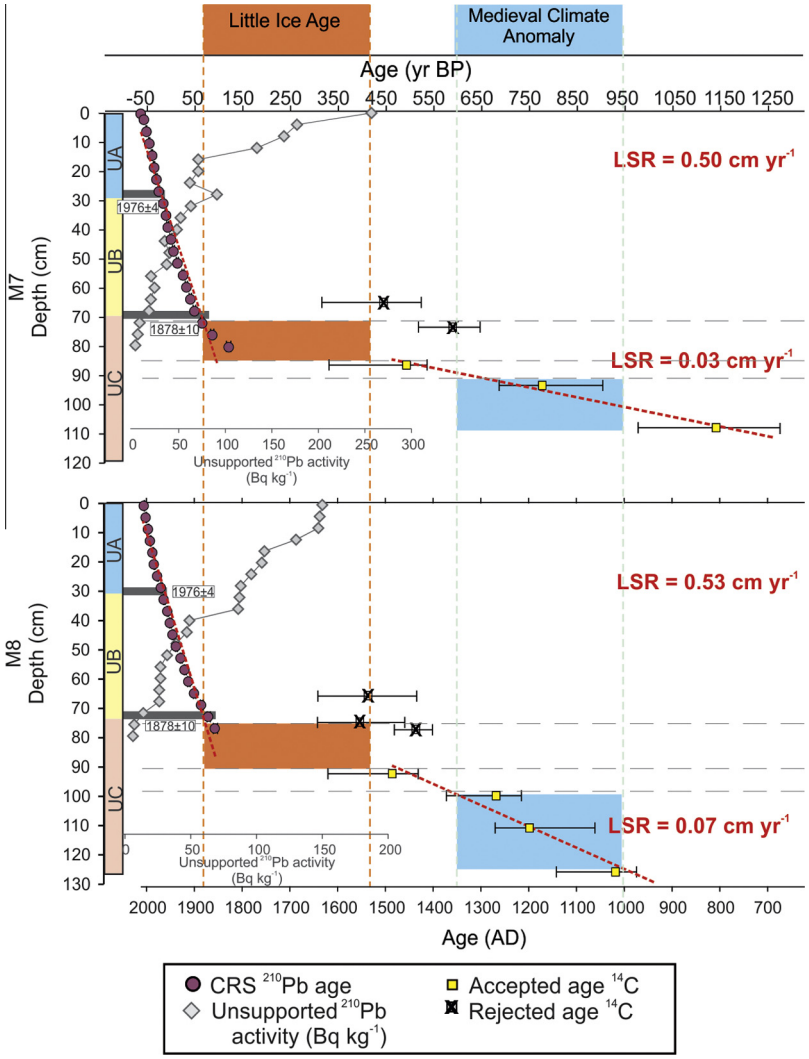

Fig. 9. Age-depth profiles showing the ^{210}Pb and ^{14}C chronological results for sediment samples from Lake Melincué. The red thick dashed lines represent the minima linear sedimentation rates (LSR). Purple circles indicate CRS model derived ages for units UA and UB. Gray diamonds represent the measured unsupported ^{210}Pb activity (Bq kg^{-1}) used in the CRS model. Yellow squares represent accepted calibrated ^{14}C ages and crossed out squares represent rejected ages. Potential hiatuses are marked by fine horizontal dashed lines. Shaded areas show the Medieval Climatic Anomaly and the Little Ice Age intervals, and the 1880 ± 10 and 1976 ± 4 humid events recognized in the Pampean Plains (Piovano et al., 2009). (For interpretation of the references to color in this figure legend, the reader is referred to the web version of this article.)

period. A major El Niño episode was reported for AD 1877–1878 (Aceituno et al., 2009) with anomalously intense rainfall and flooding events in southeastern South America. In central Argentina, intense precipitations were documented in Córdoba and catastrophic floods were registered in the coastal city of Rosario located in the Paraná River basin, close to Melincué (see location in Fig. 1B; Aceituno et al., 2009). The chronological marker assigned to AD 1878 ± 10, can also be traced in other lake sedimentary records as a comparatively positive hydrological budget during the second half of the 19th century, including a water level increase at 1878 in Mar Chiquita lake (Piovano et al., 2002; Córdoba, 2012).

Results indicate a strong agreement between the obtained CRS chronological model and the proposed age of chronostratigraphic markers in Lake Melincué records (Fig. 9). Linear regression applied for the 1832–2011 period shows a LSR of 0.50 and 0.53 cm yr^{-1} in M7B and M8B, respectively. This increment in the sedimentation rate during the deposition of UB and UA can be linked to the development of a perennial lake after the middle 19th century. In addition, by the end of the 19th century, agricultural villages were settled around the lake leading to a change in land use (H1 in Fig. 6; Pasotti et al., 1984; Biasatti et al., 1999). These combined factors could explain the increases of sedimentary flux in the perennial lacustrine system.

LSR in the upper units UA and UB from M7A and M8A show similar values. Moreover, facies limits and arrangements in both cores yield equivalent ages (Fig. 9).

6. Paleoenvironmental evolution and lake level changes during the last millennium

The analyzed sedimentary cores from Lake Melincué allow for the reconstruction of past hydrological scenarios and associated environmental variability, ranging from extremely low lake levels during dry phases to pronounced highstands at wet periods.

The environmental reconstruction reveals a first stage, which spans from 1144 ± 78 cal. yr BP/AD 806 until AD 1880 ± 3 and is represented by sediments from UC. During this stage, Lake Melincué experienced a highly fluctuating hydrological behavior, including very low to ephemeral stands and intermediate to high water level stages.

Please cite this article in press as: Guerra, L., et al. The hydrological and environmental evolution of shallow Lake Melincué, central Argentinean Pampas, during the last millennium. J. Hydrol. (2015), http://dx.doi.org/10.1016/j.jhydrol.2015.01.002

Table 2
AMS radiocarbon dates from organic rich samples obtained from M7B and M8B cores. Calibration was made with CALIB 7.0 software package (Stuiver and Reimer, 1993) using the SHCal13 calibration curve (Hogg et al., 2013). Asterisks indicate the rejected ages.

Depth (cm)	Laboratory code	Material	^{14}C AMS age (yr BP)	Calibrated age 2σ median probability (cal. yr BP)[a,b]	Calibrated age 2σ minimum (cal. yr BP)[a,b]	Calibrated age 2σ maximum (cal. yr BP)[a,b]	σ (yr)[a,b]	Age median probability (AD)[a,b]
M7B core								
*65	AA98347	Bulk sample	440 ± 62	448	319	527	64	1502
*73.5	AA98346	Bulk sample	621 ± 43	593	521	650	37	1357
86.5	AA98345	Bulk sample	474 ± 39	496	334	539	48	1454
93.5	AA98344	Bulk sample	918 ± 40	780	690	907	55	1170
108	AA98343	Bulk sample	1271 ± 64	1144	981	1278	78	806
M8B core								
*65	AA98351	Bulk sample	402 ± 65	408	303	510	64	1542
*74	AA98350	Bulk sample	354 ± 39	391	302	485	49	1559
*76.5	AA96001	Bulk sample	495 ± 35	508	463	543	28	1442
91.5	AA98349	Bulk sample	433 ± 41	458	324	513	59	1492
99	AA96002	Bulk sample	777 ± 35	676	572	729	35	1274
110	AA98348	Bulk sample	881 ± 40	746	674	883	45	1204
125	AA96003	Bulk sample	1057 ± 35	926	802	970	50	1024

[a] Calibration program: CALIB 7.0.0 Stuiver and Reimer (1993).
[b] Calibration curve: SHCal13 curve Hogg et al. (2013).

The massive and organic matter poor F5–F6 facies deposited at the base of the cores, between 1144 ± 78 cal. yr BP/AD 806 until 676 ± 35 cal. yr BP/AD 1274, indicate that the lake had a different environmental behavior than today, closer to those found in ephemeral saline lakes located in drier environments (Hardie et al., 1978; Talbot and Allen, 1996; Last, 2002; Last and Ginn, 2005; Zanor et al., 2013).

A humid phase, inferred from relative TOC increments in F6 facies at 105/115 cm level (M7B/M8B), was registered in 746 ± 45 cal. yr BP/AD 1204. This wetter pulse was contemporaneous with the MCA period defined in southeastern South America from ~AD 1100 to AD 1350 (Villalba, 1994). North and east of the Arid Diagonal (Fig. 1A), the MCA is characterized by climatic amelioration with higher temperatures and increased humidity (Cioccale, 1999; Piovano et al., 2009; Thompson et al., 2013). However, paleolimnological data from basal UC indicate that rather being uniform, this period was characterized by a marked hydroclimatic variability given by dry stages interrupted by wetter pulses. The most remarkable humid pulse recorded in UC is evidenced by the presence of organic-rich sediments from F7 facies dated by 496 ± 48 cal. yr BP/AD 1454 at 86.5 cm depth in M7B. The top of F7 is truncated by an irregular contact attributable to the development of a sedimentary hiatus; which is, in turn, followed by the deposition of F6 and F5, indicating a shift toward drier conditions. This abrupt shift from wet (F7) to dry phases (F6 and F5) could match the transition between the end of the MCA and the beginning LIA in this part of the Pampean Plains. During the LIA, temporally ascribed between ~AD 1500 and ~AD 1880 (Bradley and Jones, 1993; Bradley et al., 2003), paleoclimatic evidence suggests drier conditions with frequent extreme droughts and flood events across the Pampean region (Cioccale, 1999; Prieto and García Herrera, 2009; Stutz et al., 2010). The F6/F5 assemblage along the uppermost part of UC, spanning the period after 458 ± 59 cal. yr BP/AD 1492 up to AD 1880 (^{210}Pb age), is interpreted as the result of regional progressive drier conditions, which have also been recognized in other lake systems during the LIA (Piovano et al., 2009; Córdoba, 2012; Laprida et al., 2009; Del Puerto et al., 2013). The record of this period is poorly resolved in the Melincué sequence due to the development of sedimentary hiatuses associated to intensive droughts between AD 1492 and AD 1880. An abrupt sedimentological and geochemical change is situated between UC and UB. ^{210}Pb chronological model suggests an age of around AD 1880 for the end of the LIA. Moreover, historical chronicles denote that during AD 1779, a colonial fort was built between two small lakes (Azara, 1837; Gatti, 2010). This could represent the lake shrinking and separating into two minor bodies of water, further supporting evidence of an extremely low lake level stage. Dry conditions also characterized the first decades of the 19th century. Between AD 1827 and AD 1832, an arid episode was documented by Darwin (1860) in the central Pampas named "The Great Drought" which was responsible for dry conditions that led to massive cattle deaths, whose remains were also found in paleontological records (Tonni et al., 2008). In northern Lake Mar Chiquita, levels of evaporites are registered by this time, reflecting extremely low lake levels and regional aridity (Piovano et al., 2004a).

A striking hydrological change was registered in the basal sediments of UB by the end of the 19th century, coinciding with the beginning of the current warm period (~last 100 years; Bird et al., 2011; Thompson et al., 2013). During this period, higher sedimentary rates, continuous banding and laminations, organic matter increases and TOC/TN with algal signatures, all point to an important lake transgression (UB2) and the settlement of a perennial lake system, highly productive and deep enough to preserve sedimentary structures. Other paleoclimatological evidence based on fluvial and meteorological data suggests a high precipitation stage occurred around 1877–1878 in central Argentina (Aceituno et al., 2009). Historical contemporaneous information reveals that

Please cite this article in press as: Guerra, L., et al. The hydrological and environmental evolution of shallow Lake Melincué, central Argentinean Pampas, during the last millennium. J. Hydrol. (2015), http://dx.doi.org/10.1016/j.jhydrol.2015.01.002

villages were established near Lake Melincué near Lake Melincué at the end of the 19th century and beginning of the 20th century (Gatti, 2010). The population increase, coupled with the development of agriculture and livestock production, and its consequent land use modifications, can be considered an additional cause of increased sedimentary rates increases, nutrients input and lake eutrophication (Quirós et al., 2002).

A second short term lake transgression is noted in the basal sediments of the subunit UB1 dating from AD 1914 (^{210}Pb date), coeval with a high precipitation phase, which is also evident in the instrumental records (Fig. 2A). Toward the top of the subunit, increased carbonate and reduced organic matter proportions indicate a gradual lake shrinking, following the instrumental water level data (Fig. 2B). This led to a new state of shallow saline lake that lasted until the middle 1970s.

At the base of UA, an important water level rise is inferred from notable organic matter percentages increases, finer grain-sized sediments and salinity drops (as noted by low carbonate amounts). This period corresponds to the development of a perennial, high-level, subsaline lake. The highstand event produced important documented village flooding after AD 1975 (Pasotti et al., 1984). The rising lake levels are linked to the high precipitation interval that started during the 1970s and lasted until AD 2004 (Fig. 2A and B). This wet spell is sharply manifested in other hydrological systems in central Argentina (e.g. Piovano et al., 2002, 2004a, 2004b; Pasquini et al., 2006; Córdoba, 2012). Alternating F1–F2 deposition in UA is a consequence of short-lived pulses of highly variable water lake-level conditions, but in a perennial subsaline lake, deep enough to preserve lamination. Increased productivity during this period can be associated with the higher water levels, and also with the potential effect of an agricultural expansion that started in the region after the 1970s (Viglizzo and Jobbágy, 2010). Finally, the top of the unit corresponds to the present sediment deposition under a shallow subsaline lake in AD 2011.

7. Conclusions

Lake Melincué is a highly variable lacustrine system. The development of the associated subenvironments is conditioned to the lake's water level, which is largely dependent upon the hydrological balance. The present-day shallow subsaline lake corresponds to a lowstand situation. In this system, different depositional subenvironments have developed, including inner and marginal lacustrine areas, along with mudflats, vegetated mudflats and wetlands in the supralittoral areas.

The sedimentary record of Lake Melincué provides a high resolution paleohydrological reconstruction of the central Pampean Plains during the last millennium. The combined analyses of sedimentary facies, physical and geochemical data allowed the identification of three sedimentary units that represent contrasting stages of the environmental evolution.

The period spanning from AD 806 to AD 1880, represented by massive and predominantly sediments poor in organic matter (terrestrial plant sources) sediments from UC, was characterized by important lake level fluctuations. From AD 806 to AD 1274, previous to and synchronous with the MCA, Lake Melincué had a different environmental behavior than today, with extremely low water levels, representative of ephemeral to a very shallow lake in a drier environment interrupted by relatively wetter phases. An important humid event was represented by the organic F7 facies, at the MCA–LIA transition (~AD 1450/92). A hyper-arid period, characterized by extremely low lake levels and possible lake floor exposures, developed after F7 deposition and lasted until the end of the LIA. After AD 1880 (UB), a pronounced shift to increased algal production and well-laminated sediments is interpreted as the result of an important lacustrine transgression and the settlement of a perennial lake, coinciding with the beginning of the current warm period. The onset of this period is synchronous in several climatic records in southern South America. High sedimentation rates and internal productivity could have been enhanced by changes in land use since the end of the 18th century.

The early to mid-20th century was characterized by dominant low lake levels corresponding to dry conditions. After AD 1975, the lake underwent a striking expansion (UA), following regional hydrological and precipitation increases that have also been detected in the instrumental records. The highstand provoked floods with catastrophic consequences for lake-shore villages and surrounding infrastructure. Humid conditions extended until 2004, when the lake started to recede as a consequence of decreased regional precipitation patterns, ruling the expansion of the supralittoral subenvironments.

Achieved paleoenvironmental reconstruction highlights the value of Lake Melincué as a high quality archive of past hydrological changes. These results will contribute to the complete picture of hydroclimatic evolution and the activity of the SAM during the last millennium across southeastern South America, as well as to the analysis of the most recent hydroclimatic change within a larger time-window covering the last 1000 years.

Acknowledgements

The research was supported by a PhD Grant from CONICET – Argentina (Lucía Guerra). Different aspects of the results presented here have been carried out at CICTERRA (CONICET/Universidad de Córdoba, Argentina), CEREGE (Centre Européen de Recherche et d'Enseignement des Géosciences de l'Environnement, Aix en Provence, France) and IPEN (Instituto de Pesquisas Energéticas e Nucleares, Sao Paulo, Brasil). This study was partially funded by CONICET (PIP 2012-2014/11220110100759), SECYT-UNC (2012-2013), PID-2008 (Ministerio de Ciencia y Tecnología de la Provincia de Córdoba), European Community's Seventh Framework Programme (FP7/2007-2013) under Grant Agreement N° 212492: CLARIS LPB, "A Europe-South America Network for Climate Change Assessment and Impact Studies in La Plata Basin".

Special appreciations must be given to the firemen from the Asociación de Bomberos Voluntarios from Melincué for their valuable help in the field work. A special acknowledgement is also given to Frauke Rostek, for her intense guidance and help in the laboratory work at CEREGE.

References

Aceituno, P., del Rosario Prieto, M., Solari, M.E., Martínez, A., Poveda, G., Falvey, M., 2009. The 1877–1878 El Niño episode: associated impacts in South America. Clim. Change 92 (3–4), 389–416.

Adrian, R. et al., 2009. Lakes as sentinels of current climate change. Limnol. Oceanogr. 54, 2283–2297.

Appleby, P.G., 2008. Three decades of dating recent sediments by fallout radionuclides: a review. The Holocene 18 (1), 83–93.

Appleby, P.G., Oldfield, F., 1978. The calculation of lead-210 dates assuming a constant rate of supply of unsupported/mPb to the sediment. Catena 5, 1–8.

Arnaud, F., Lignier, V., Revel, M., Desmet, M., Beck, C., Pourchet, M., Charlet, F., Tribovillard, N., 2002. Flood and earthquake disturbance of ^{210}Pb geochronology (Lake Anterne, NW Alps). Terra Nova 14 (4), 225–232.

Azara, F., 1837. Diario de un reconocimiento de las guardias y fortines, que guarnecen la línea de frontera de Buenos-Aires para ensancharla. Imprenta del Estado, Buenos Aires, 49 pp.

Biasatti, N., Delannoy, L., Peralta, E., Pire, E., Romano, M., Torres, G., 1999. Cuenca Hidrográfica del Humedal de la Laguna Melincué, Provincia de Santa Fe. ProDIA, SRNyDS, Buenos Aires.

Binford, M.W., 1990. Calculation and uncertainty analysis of ^{210}Pb dates for PIRLA project lake sediment cores. J. Paleolimnol. 3 (3), 253–267.

Bird, B.W., Abbott, M.B., Vuille, M., Rodbell, D.T., Stansell, N.D., Rosenmeier, M.F., 2011. A 2,300-year-long annually resolved record of the South American summer monsoon from the Peruvian Andes. Proc. Natl. Acad. Sci. 108 (21), 8583–8588.

Bradley, R.S., Jones, P.D., 1993. 'Little Ice Age' summer temperature variations: their nature and relevance to recent global warming trends. The Holocene 3 (4), 367–376.

Bradley, R.S., Briffa, K.R., Cole, J., Hughes, M.K., Osborn, T.J., 2003. The climate of the last millennium. In: Paleoclimate, Global Change and the Future. Springer, Berlin, Heidelberg, pp. 105–141.

Brunetto, E., Iriondo, M., Zamboni, L., Gottardi, G., 2010. Quaternary deformation around the Palo Negro area, Pampa Norte, Argentina. J. S. Am. Earth Sci. 29 (3), 627–641.

Bruniard, E.D., 1982. La diagonal árida Argentina: un límite climático real. Rev. Geogr., 5–20

Cioccale, M.A., 1999. Climatic fluctuations in the Central Region of Argentina in the last 1000 years. Quatern. Int. 62 (1), 35–47.

Córdoba, F., 2012. El registro climático del Holoceno tardío en latitudes medias del SE de Sudamérica: limnogeología de las Lagunas Encadenadas del Oeste, Argentina. PhD Thesis, Universidad Nacional de Córdoba, 285 pp.

da Silva, L.S.V., Piovano, E.L., Azevedo, D.D.A., Aquino Neto, F.R.D., 2008. Quantitative evaluation of sedimentary organic matter from Laguna Mar Chiquita, Argentina. Org. Geochem. 39 (4), 450–464.

Darwin, C., 1860. A Naturalist's Voyage Round the World. The Voyage of the Beagle, first ed., pp. 142–143 (The Project Gutenberg EBook). <http://www.darwinsgalapagos.com/Darwin_voyage_beagle/darwin_beagle_title.html> (Chapter VII).

Dávila, F.M., Lithgow-Bertelloni, C., Giménez, M., 2010. Tectonic and dynamic controls on the topography and subsidence of the Argentine Pampas: the role of the flat slab. Earth Planet. Sci. Lett. 295 (1), 187–194.

Dearing, J., 1994. Environmental Magnetic Susceptibility. Using the Bartington MS2 System. Chi Publ., Kenilworth.

Dearing, J.A., 1999. Holocene environmental change from magnetic proxies in lake sediments. In: Maher, B., Thompson, R. (Eds.), Quaternary Climates, Environments and Magnetism. Cambridge University Press, United Kingdom, pp. 231–278.

Del Puerto, L.D., Bracco, R., Inda, H., Gutiérrez, O., Panario, D., García-Rodríguez, F., 2013. Assessing links between late Holocene climate change and paleolimnological development of Peña Lagoon using opal phytoliths, physical, and geochemical proxies. Quatern. Int. 287, 89–100.

Eugster, H.P., 1980. Geochemistry of evaporitic lacustrine deposits. Annu. Rev. Earth Planet. Sci. 8, 35.

Garreaud, R.D., Vuille, M., Compagnucci, R., Marengo, J., 2009. Present-day South American climate. Palaeogeogr. Palaeoclimatol. Palaeoecol. 281 (3), 180–195.

Gatti, S., 2010. Melincué, su historia. Biblioteca Popular Bernardino Rivadavia, first ed. Melincué, Santa Fe, Argentina.

Hardie, L.A., Smoot, J.P., Eugster, H.P., 1978. Saline Lakes and their Deposits: A Sedimentological Approach. Modern and Ancient Lake Sediments. International Association of Sedimentologists, Special Publication No. 2, pp. 7–42.

Hogg, A.G., Hua, Q., Blackwell, P.G., Niu, M., Buck, C.E., Guilderson, T.P., Heaton, T.J., Palmer, J.G., Reimer, P.J., Reimer, R.W., Turney, C.S.M., Zimmerman, S.R., 2013. Shcal13 Southern Hemisphere calibration, 0–50,000 years Cal BP. Radiocarbon 55 (4).

Iriondo, M., 1989. Quaternary lakes of Argentina. Palaeogeogr. Palaeoclimatol. Palaeoecol. 70 (1), 81–88.

Iriondo, M., Kröhling, D., 2007. Geomorfología y sedimentología de la cuenca superior del río Salado (sur de Santa Fe y noroeste de Buenos Aires, Argentina). Latin Am. J. Sediment. Basin Anal. 14 (1), 1–23.

Jarvis, A., Reuter, H.I., Nelson, A., Guevara, E., 2008. Hole-filled Seamless SRTM Data V4. International Centre for Tropical Agriculture (CIAT), <http://srtm.csi.cgiar.org>.

Jones, P.D., Hulme, M., 1996. Calculating regional climatic time series for temperature and precipitation: methods and illustrations. Int. J. Climatol. 16, 361–377.

Karlin, R., Levi, S., 1983. Diagenesis of magnetic minerals in recent haemipelagic sediments. Nature 303 (5915), 327–330.

Kröhling, D.M., 1999. Upper quaternary geology of the lower Carcarañá Basin, North Pampa, Argentina. Quatern. Int. 57, 135–148.

Laprida, C., Orgeira, M.J., García Chapori, N., 2009. El registro de la Pequeña Edad de Hielo en lagunas pampeanas. Rev. Asoc. Geol. Argentina 65 (4), 603–611.

Last, W.M., 2002. Geolimnology of salt lakes. Geosci. J. 6 (4), 347–369.

Last, W.M., Ginn, F.M., 2005. Saline systems of the Great Plains of western Canada: an overview of the limnogeology and paleolimnology. Saline Syst. 1 (1), 10.

Mayr, C., Fey, M., Haberzettl, T., Janssen, S., Lücke, A., Maidana, N.I., Ohlendorf, C., Schäbitz, F., Schleser, G.H., Struck, U., Wille, M., Zolitschka, B., 2005. Palaeoenvironmental changes in southern Patagonia during the last millennium recorded in lake sediments from Laguna Azul (Argentina). Palaeogeogr. Palaeoclimatol. Palaeoecol. 228 (3), 203–227.

Meyers, P.A., 1994. Preservation of elemental and isotopic source identification of sedimentary organic matter. Chem. Geol. 114 (3), 289–302.

Meyers, P.A., 2003. Applications of organic geochemistry to paleolimnological reconstructions: a summary of examples from the Laurentian Great Lakes. Org. Geochem. 34 (2), 261–289.

Meyers, P.A., Lallier-Vergès, E., 1999. Lacustrine sedimentary organic matter records of Late Quaternary paleoclimates. J. Paleolimnol. 21 (3), 345–372.

Meyers, P.A., Teranes, J.L., 2002. Sediment organic matter. In: Last, W.M., Smol, J.P. (Eds.), Tracking Environmental Change using Lake Sediments: Physical and Geochemical Methods. Springer, The Netherlands, pp. 239–269.

Moreira, S.R.D., 1993. Determinação de 210Pb em Águas Minerais da Cidade de Águas da Prata. Unpubl. MSc Thesis, Instituto de Pesquisas Energéticas e Nucleares, Sao Paulo, Brazil, 86 pp.

Moreno, A., Giralt, S., Valero-Garcés, B., Sáez, A., Bao, R., Prego, R., Pueyo, J.J., González-Sampériz, P., Taberner, C., 2007. A 14 kyr record of the tropical Andes: the Lago Chungará sequence (18°S, northern Chilean Altiplano). Quatern. Int. 161 (1), 4–21.

Oliveira, J., 1993. Determinação de 226Ra e 228Ra em Á guas Minerais da Região de Águas da Prata. Unpubl. MSc Thesis, Instituto de Pesquisas Energéticas e Nucleares, Sao Paulo, Brazil, 86 pp.

Pasotti, P., Albert, O., Canoba, C.A., 1984. Contribución al conocimiento de la laguna Melincué. Universidad Nacional de Rosario, Facultad de Exactas e Ingeniería, Instituto de Fisiografía y Geología.

Pasquini, A.I., Lecomte, K.L., Piovano, E.L., Depetris, P.J., 2006. Recent rainfall and runoff variability in central Argentina. Quatern. Int. 158 (1), 127–139.

Peralta, E., Romano, M., Delannoy, L., Biasatti, N.R., 2003. Manejo integrado de cuencas hidrográficas. Caso de estudio: La laguna Melincué, Problemática y Perspectivas. Ambiental 4, 90–105.

Piovano, E.L., Ariztegui, D., Moreira, S.D., 2002. Recent environmental changes in Laguna Mar Chiquita (central Argentina): a sedimentary model for a highly variable saline lake. Sedimentology 49 (6), 1371–1384.

Piovano, E.L., Ariztegui, D., Bernasconi, S.M., McKenzie, J.A., 2004a. Stable isotopic record of hydrological changes in subtropical Laguna Mar Chiquita (Argentina) over the last 230 years. The Holocene 14 (4), 525–535.

Piovano, E.L., Larizzatti, F.E., Fávaro, D.I., Oliveira, S.M., Damatto, S.R., Mazzilli, B.P., Ariztegui, D., 2004b. Geochemical response of a closed-lake basin to 20th century recurring droughts/wet intervals in the subtropical Pampean Plains of South America. J. Limnol. 63 (1), 21–32.

Piovano, E.L., Ariztegui, D., Córdoba, F., Cioccale, M., Sylvestre, F., 2009. Hydrological variability in South America below the Tropic of Capricorn (Pampas and Patagonia, Argentina) during the last 13.0 Ka. In: Past Climate Variability in South America and Surrounding Regions. Springer, Netherlands, pp. 323–351.

Prieto, M.D.R., García Herrera, R., 2009. Documentary sources from South America: potential for climate reconstruction. Palaeogeogr. Palaeoclimatol. Palaeoecol. 281 (3), 196–209.

Quirós, R., Drago, E., 1999. The environmental state of Argentinean lakes: an overview. Lakes Reserv.: Res. Manage. 4 (1–2), 55–64.

Quirós, R., Rennella, A.M., Boveri, M.A., Rosso, J.J., Sosnovsky, A., 2002. Factores que afectan la estructura y el funcionamiento de las lagunas pampeanas. Ecol. Austral 12 (2), 175–185.

Robbins, J.A., 1978. Geochemical and geophysical applications of radioactive lead. Biogeochemistry of lead in the environment 1, 285–337.

Romano, M., Barberis, I., Pagano, F., Maidagan, J., 2005. Seasonal and interannual variation in waterbird abundance and species composition in the Melincué saline lake, Argentina. Eur. J. Wildl. Res. 51 (1), 1–13.

Sanchez-Cabeza, J.A., Ruiz-Fernández, A.C., 2012. ^{210}Pb sediment radiochronology: an integrated formulation and classification of dating models. Geochim. Cosmochim. Acta 82, 183–200.

Steinman, B.A., Abbott, M.B., 2013. Isotopic and hydrologic responses of small, closed lakes to climate variability: hydroclimate reconstructions from lake sediment oxygen isotope records and mass balance models. Geochim. Cosmochim. Acta 105, 342–359.

Stuiver, M., Reimer, P.J., 1993. Extended (super 14) C data base and revised CALIB 3.0 (super 14) C age calibration program. Radiocarbon 35 (1), 215–230.

Stutz, S., Borel, C.M., Fontana, S.L., del Puerto, L., Inda, H., García-Rodriguez, F., Tonello, M.S., 2010. Late Holocene climate and environment of the SE Pampa grasslands, Argentina, inferred from biological indicators in shallow, freshwater Lake Nahuel Rucá. J. Paleolimnol. 44 (3), 761–775.

Stutz, S., Borel, C.M., Fontana, S.L., Tonello, M.S., 2012. Holocene changes in trophic states of shallow lakes from the Pampa plain of Argentina. The Holocene 22 (11), 1263–1270.

Talbot, M.R., Allen, P.A., 1996. Lakes. In: Reading, H.G. (Ed.), Sedimentary Environments: Processes, Facies and Stratigraphy, third ed. Blackwell Science, Oxford, pp. 83–124.

Thompson, L.G., Mosley-Thompson, E., Dansgaard, W., Grootes, P.M., 1986. The Little Ice Age as recorded in the stratigraphy of the tropical Quelccaya ice cap. Science 234 (4774), 361–364.

Thompson, L.G., Mosley-Thompson, E., Davis, M.E., Zagorodnov, V.S., Howat, I.M., Mikhalenko, V.N., Lin, P.N., 2013. Annually resolved ice core records of tropical climate variability over the past ~1800 years. Science 340 (6135), 945–950.

Tonni, E.P., Bonini, R.A., Molinari, A.E., Prevosti, F.J., Pomi, L.H., Carbonari, J.E., Huarte, R., 2008. Análisis radiocarbónico en una tafocenosis de la región pampeana (provincia de Buenos Aires, Argentina): su vinculación con la Gran Seca de 1827–1832. Inters. Antropol. 9, 307–311.

Valero-Garcés, B.L., Delgado-Huertas, A., Navas, A., Edwards, L., Schwalb, A., Ratto, N., 2003. Patterns of regional hydrological variability in central-southern Altiplano (18–26S) lakes during the last 500 years. Palaeogeogr. Palaeoclimatol. Palaeoecol. 194 (1), 319–338.

Vera, C., Higgins, W., Amador, J., Ambrizzi, T., Garreaud, R., Gochis, D., Gochis, D., Gutzler, D., Lettenmaier, D., Marengo, J., Mechoso, C.R., Nogues-Paegle, J., Silva Dias, P.L., Zhang, C., 2006. Toward a unified view of the American monsoon systems. J. Clim. 19 (20).

Verardo, D.J., Froelich, P.N., McIntyre, A., 1990. Determination of organic carbon and nitrogen in sediments using the Carlo Erba N-1500 analyser. Deep Sea Res. 37 (1), 157–165.

Viglizzo, E., Jobbágy, E.G., 2010. Expansión de la frontera agropecuaria en Argentina y su impacto ecológico-ambiental. Ediciones INTA, Buenos Aires.

Please cite this article in press as: Guerra, L., et al. The hydrological and environmental evolution of shallow Lake Melincué, central Argentinean Pampas, during the last millennium. J. Hydrol. (2015), http://dx.doi.org/10.1016/j.jhydrol.2015.01.002

Villalba, R., 1994. Tree-ring and glacial evidence for the Medieval Warm Epoch and the Little Ice Age in southern South America. In: The Medieval Warm Period. Springer, Netherlands, pp. 183–197.

Villalba, R., Grosjean, M., Kiefer, T., 2009. Long-term multi-proxy climate reconstructions and dynamics in South America (LOTRED-SA): state of the art and perspectives. Palaeogeogr. Palaeoclimatol. Palaeoecol. 281 (3), 175–179.

Von Gunten, L., Grosjean, M., Beer, J., Grob, P., Morales, A., Urrutia, R., 2009. Age modeling of young non-varved lake sediments: methods and limits. Examples from two lakes in Central Chile. J. Paleolimnol. 42 (3), 401–412.

Zanor, G.A., Piovano, E.L., Ariztegui, D., Pasquini, A.I., Chiesa, J.O., 2013. El registro sedimentario Pleistoceno tardío-Holoceno de la Salina de Ambargasta (Argentina central): una aproximación paleolimnológica. Rev. Mexicana Ciencias Geol. 30 (2), 336–354.

Zhou, J., Lau, K.M., 1998. Does a monsoon climate exist over South America? J. Clim. 11 (5).

Zhou, J., Lau, K.M., 2001. Principal modes of interannual and decadal variability of summer rainfall over South America. Int. J. Climatol. 21 (13), 1623–1644.

Please cite this article in press as: Guerra, L., et al. The hydrological and environmental evolution of shallow Lake Melincué, central Argentinean Pampas, during the last millennium. J. Hydrol. (2015), http://dx.doi.org/10.1016/j.jhydrol.2015.01.002